Journal of Colloid and Interface Science xxx (2012) xxx–xxx

Contents lists available at SciVerse ScienceDirect

Journal of Colloid and Interface Science

www.elsevier.com/locate/jcis

A comparative study of in-flow and micro-patterning biofunctionalization protocols for nanophotonic silicon-based biosensors

Ana Belén González-Guerrero [a], Mar Alvarez [a], Andrés García Castaño [b], Carlos Domínguez [b], Laura M. Lechuga [a,*]

[a] Nanobiosensors and Bioanalytical Applications Group, Research Center on Nanoscience and Nanotechnology (CIN2), CSIC and CIBER-BBN, Barcelona, Spain
[b] Microelectronics Institute of Barcelona (IMB-CNM), CSIC, Barcelona, Spain

ARTICLE INFO

Article history:
Received 6 September 2012
Accepted 19 October 2012
Available online xxxx

Keywords:
Biofunctionalization
Photonic biosensors
Micro-patterning
Silicon interferometers
CTES
Aqueous-silane

ABSTRACT

Reliable immobilization of bioreceptors over any sensor surface is the most crucial step for achieving high performance, selective and sensitive biosensor devices able to analyze human samples without the need of previous processing. With this aim, we have implemented an optimized scheme to covalently biofunctionalize the sensor area of a novel nanophotonic interferometric biosensor. The proposed method is based on the ex-situ silanization of the silicon nitride transducer surface by the use of a carboxyl water soluble silane, the carboxyethylsilanetriol sodium salt (CTES). The use of an organosilane stable in water entails advantages in comparison with usual trialkoxysilanes such as avoiding the generation of organic waste and leading to the assembly of compact monolayers due to the high dielectric constant of water. Additionally, cross-linking is prevented when the conditions (e.g. immersion time, concentration of silane) are optimized. This covalent strategy is followed by the bioreceptor linkage on the sensor area surface using two different approaches: an in-flow patterning and a microcontact printing using a biodeposition system. The performance of the different bioreceptor layers assembled is compared by the real-time and label-free immunosensing of the proteins BSA/mAb BSA, employed as a model molecular pair. Although the results demonstrated that both strategies provide the biosensor with a stable biological interface, the performance of the bioreceptor layer assembled by microcontact printing slightly improves the biosensing capabilities of the photonic biosensor.

1. Introduction

The past few years have witnessed a significant progress in the development of biosensing devices based on silicon photonics. These devices can offer several advantages over traditional methodologies, such as ELISA or RIA test, which are time-consuming, expensive, and need from bulky instrumentation usually located in laboratory environments. Photonic biosensors based on evanescent wave detection are able to perform highly sensitive detections in a label-free scheme providing rapid, affordable, and simple analysis. Among evanescent wave optical biosensors, interferometric ones are recognized to be one of the most sensitive devices for label-free analysis [1]. Moreover, they can be fabricated with standard silicon technology affording mass production and miniaturization which make interferometric devices suitable candidates for providing a multiplexed and portable analytical tool.

However, the sensitivity of a biosensing platform is a complex parameter, directly related to the transducer sensing principle, but strongly dependent of other parameters such as the material, working wavelength, surface cleanness, protein surface coverage, and biorecognition method. A reliable immobilization of bioreceptors over any sensor surface is the most crucial step for achieving high performance, selective, and sensitive biosensors able to analyze human samples directly, without the need of previous processing. Integrated nanophotonic devices commonly use silicon nitride (Si_3N_4) as core layer due to its high refractive index that allows the confinement of light. Additionally, Si_3N_4 has excellent properties to be an optimal sensing area surface such as high density and chemical inertness that make it resistant to ion species, oxygen, and moisture permeation [2]. Covalent attachment of molecules to this surface is preferred due to its long-term stability in fluid systems allowing the biosensor to be reused several times [3]. However, the covalent strategy is more complex than physical adsorption [4] implying the modification of the Si_3N_4 surface by incorporating functional groups able to react with the biomolecules. Among the available functional groups, carboxyl groups are the most suitable candidates in order to conjugate proteins to surfaces [5–7]. Several strategies to provide silicon-based surfaces with carboxyl groups have been reported: via the attachment of

* Corresponding author. Fax: +34 93 586 80 20.
E-mail address: Laura.lechuga@cin2.es (L.M. Lechuga).

0021-9797/$ - see front matter © 2012 Elsevier Inc. All rights reserved.
http://dx.doi.org/10.1016/j.jcis.2012.10.040

a trifluoro ethanol ester and subsequent thermal acid hydrolysis, or through the attachment of a photocleavable ester and subsequent photochemical cleavage [5], besides via the attachment of long-chain carboxylic acid terminated monolayers [6,7]. However, these strategies involve a large number of steps, require of additional instrumentation, and are time-consuming.

Silanization methods are the simplest and most common way to covalently modify silicon-based surfaces and have been extensively reviewed in the literature [8]. Organofunctional trialkoxysilanes (such as 3-aminopropyltriethoxy (APTES) silane [9] and the 3-trimethoxysilyil propyl methacrylate (MPTS) silane [10]) are the most employed for liquid-phase silanization. An undesirable effect regarding the use of trialkoxysilanes is the polymerization that can occur at the free silanol groups on the surface or in solution, leading to highly heterogeneous surfaces, a potential disadvantage when dealing with biosensors. To avoid this negative effect, anhydrous solvents have been used to limit the amount of water reacting during the monolayer formation [11]. However, small variations in the amount of water during the silanization reaction can dramatically alter the thickness of the final film giving place to highly irreproducible surfaces due to the formation of silane multilayers [9].

To achieve a carboxylic acid terminated layer on the Si_3N_4 surface by a simple silanization method, avoiding the derived problems of using anhydrous solvents, we chose to study the use of a carboxyethylsilanetriol sodium salt (CTES). This aqueous soluble silane is extensively used for the functionalization of silica particles [12,13] and as a co-structure directing agent [14]. In spite of its wide use for the synthesis of particles, few works can be found about functionalization of silicon surfaces with CTES silane [15]. Due to its short alkyl chain of approximately 6 Å and to the hydrophilicity of the functional carboxyl group that contains, CTES is an organosilane stable front the cross-linking in water. This is an unusual property for a silane molecule that makes the use of CTES especially attractive to avoid concerns regarding the use of organic solvents and the generation of organic waste by the rinsing steps. Another attractive aspect of the use of water as solvent for the reaction is its larger dielectric constant, which favors the formation of packaged monolayers [16]. Moreover, the solvent compatibility with the polymer materials employed in our fluidic systems allows the use of CTES to silanize the sensor area inside the fluidic cell (in-flow) when necessary for specific applications.

Another important issue related with the formation of a bioreceptor layer is the method employed to place the biomolecules on the sensor surface. The most explored methods for the immobilization of the bioreceptor layer in biosensors are the in-flow strategy [17] and the patterning of surfaces [18]. The in-flow strategy uses smalls channels with low Reynolds number that generates a laminar flow [19], and allows the real-time monitoring of the layer formation. On the other hand, the surface patterning is based on the selective deposition of small volumes of samples under static conditions, which avoids the formation of the typical geometrical patterns due to the laminar flow [17].

In this work, we report the functionalization of the Si_3N_4 surface of a nanophotonic biosensor with carboxyl groups by an organosilane molecule stable in water. We found out the optimum reaction parameters (time and concentration) and the resulting film morphology of the carboxylic acid terminated CTES silane monolayer on Si_3N_4 test surfaces by using standard techniques such as contact angle characterization, atomic force microscopy (AFM), and fluorescent analysis. After that, the optimized silanization protocol was applied to the sensor area surface of a Bimodal Waveguide device (BiMW) to evaluate its biosensing capabilities by using the proteins BSA/mAb BSA as a model molecular pair. Both immobilization strategies, in-flow and micropatterning of surfaces, were applied to the BiMW sensors for comparison. The main goal of this work was not only to find out the optimized parameters for a new silanization method based on an organosilane stable in water but also to assess its application with two different protein immobilization methods for nanophotonic biosensing applications.

2. Materials and methods

2.1. Materials

Carboxyethylsilanetriol sodium salt (CTES) was purchased from ABCR, Germany. Ethanol (EtOH, 99%), acetone (Ac, 99.5%), hydrochloric acid (HCl, 35–38%), and methanol (MeOH, 99.5%) were purchased from Panreac, Spain. Sodium dodecyl sulfate (SDS) (99%), albumin bovine serum (BSA), albumin fluorescein isothiocyanate conjugate bovine (FTIC-BSA), components for the phosphate buffer saline (PBS; 10 mM phosphate, 2.9 mM KCl, 137 mM NaCl, pH 7.4) and for the tris(hydroxymethyl)amino methane buffer (TRIS; 10 mM, pH 7.1), N-hydroxysuccinimide (NHS, 98%), monoclonal antibovine serum albumin antibody (mAb BSA) and, N-(3-dimethylaminopropyl)-N′-ethylcarbodiimide hydrochloride (EDC) were purchased from Sigma–Aldrich, Germany. DI water from Millipore, USA, was always employed. Polydimethylsiloxane (PDMS) was purchased from Dow Corning, Germany.

2.2. Si_3N_4 test surfaces

The Si_3N_4 test surfaces consist of: a silicon dioxide layer (2 μm thickness) thermally grown over a silicon wafer (500 μm thickness), followed by a Si_3N_4 layer of 180 nm thickness deposited by low pressure chemical vapor deposition (LPCVD) technique. Wafer was diced into 1 cm^2 square pieces for the silanization experiments.

2.3. Biodeposition platform

A NanoeNablerTM system (BioForce Nanosciences, USA) was employed for the selective deposition of FTIC-BSA solution on the pretreated Si_3N_4 test surfaces and the BiMW sensor areas. This molecular printing platform enables the direct writing/deposition of 1–60 μm size droplets with a high position resolution (20 nm *X*, *Y*, and *Z* resolution). The size of the deposited drops depends on the contact time and force between the Surface Patterning Tool (SPT) cantilever and the surface being patterned, which are controlled by using a variable intensity laser and a position-sensitive photodetector. Molecules to be printed are loaded into the reservoirs of the SPT cantilevers by using a pipette (0.5 μl). In this work, SPT tools with rounded edge and 30 μm width were used (SPT-S-C30R). The SPT tools were previously cleaned with hot organic solvents and under UV/Ozone cleaner (UV/Ozone ProCleaner TM, BioForce Nanosciences, USA) during at least 40 min, to facilitate wettability and fluid flow though the cantilever. Glycerol is normally used to facilitate the filling of the cantilever channel and to reduce evaporation of the drops. Relative humidity is adjusted to 50%, and after the spotting the chip was incubated for 1 h, at room temperature and 50% ambient humidity, to achieve a uniform covalent linked protein layer.

2.4. Contact angle analysis

The analysis of the drop shape was done with an Easy drop standard apparatus (Krüss, Hamburg). The contact angle technique is a quick, inexpensive, and efficient method to get an immediate evaluation of the efficiency of a surface biomodification. In fact, the low values of contact angles corresponding to cleaned/oxidized surfaces (hydrophilic surface) dramatically increase after a protein

attachment process (hydrophobic surface). Drops of 3 μl volume were placed on the Si_3N_4 surface for the analysis. Each reported result corresponds to the average of 10 different measurements.

2.5. Analysis by atomic force microscopy

AFM images were recorded with an Agilent 5500 AFM/SPM microscope (formerly molecular Imaging PicoPlus AFM) in tapping mode. A multi-purpose low-coherence scanner with scan range up to 90 μm was used for imaging the samples under ambient conditions. The AFM probes were NSC15 silicon pointprobes (force constant 30–50 N/m, resonant frequency 330 KHz) from MikroMasch, Estonia. AFM images processing was done with the WSxM software (Nanotec, Spain) [20]. Surface roughness was obtained by evaluating the vertical deviation from the average value.

2.6. Fluorescent analysis

Fluorescence analysis of the patterned surfaces was carried out by using an inverted microscope (TE 2000U Nikon, Spain) and a filter set for Cy3TM (Chroma Technology, USA). Images of the same experiment were taken with the same parameters of camera exposition for a reliable comparison.

2.7. BiMW sensor

The functionalization protocols developed in this work were investigated using a nanophotonic biosensor previously developed in our group, based on a bimodal waveguide [21]. The BiMW transducer has already demonstrated an extremely low detection limit for detection of bulk solutions (LOD: 2.5×10^{-7} Refractive Index Units, RIU). The BiMW biosensor working principle, sketched in Fig. 1a, is based on the evanescent field variations which allows the detection of analytes in real-time and free of labels. The bimolecular interaction between the analyte to detect and the corresponding bioreceptor immobilized on the waveguide surface within the evanescent field region results in a variation of the refractive index of the waveguide outer medium. This modification affects the effective index of the wave propagating through the waveguide. The BiMW device consists of a straight Si_3N_4 nanometric rib waveguide in which the sensing mechanism is based on the interference of two modes with the same polarization. The propagating modes are induced by an abrupt increase of the height of the waveguide core which transforms the waveguide from single-mode (150 nm) to bimodal (340 nm) as can be seen in Fig. 1b. The fundamental mode is more confined in the core than the first excited mode; therefore the biorecognition event occurring on the sensor area surface will affect differently both modes through their evanescent field, generating and interference pattern at the output of the waveguide that can be related with the concentration of analyte.

The devices were fabricated at wafer level using standard microelectronics technology at our Clean Room facilities. The total length of the chip was 30 mm. The length of the bimodal part was 25 mm, which includes the sensing window with a length of 15 mm, placed 5 mm off the chip exit. The sensor area (50 μm width and 2 μm height) was opened in the upper SiO_2 cladding layer in order to expose the Si_3N_4 rib waveguide to the external medium. The final chip (see Fig. 1c) was $30 \times 10\ mm^2$ in size and contained 16 independent BiMW sensors with a pitch of 250 μm between them. The rib of the waveguide has a width of 4 μm and a height of 1.2 nm. An Atomic Force Microscope image (AFM) of the rib waveguide is shown in Fig. 1c.

For the biosensing evaluation, a poly(methyl methacrylate) (PMMA) fluidic cell was fabricated and coupled to the sensor chip as can be seen in Fig. 1d. The fluidic cell contains four fluidics channels with a pitch of 1 mm between them. Each channel has a length of 18 mm, a height of 0.5 mm, and a width of 1.5 mm, which means

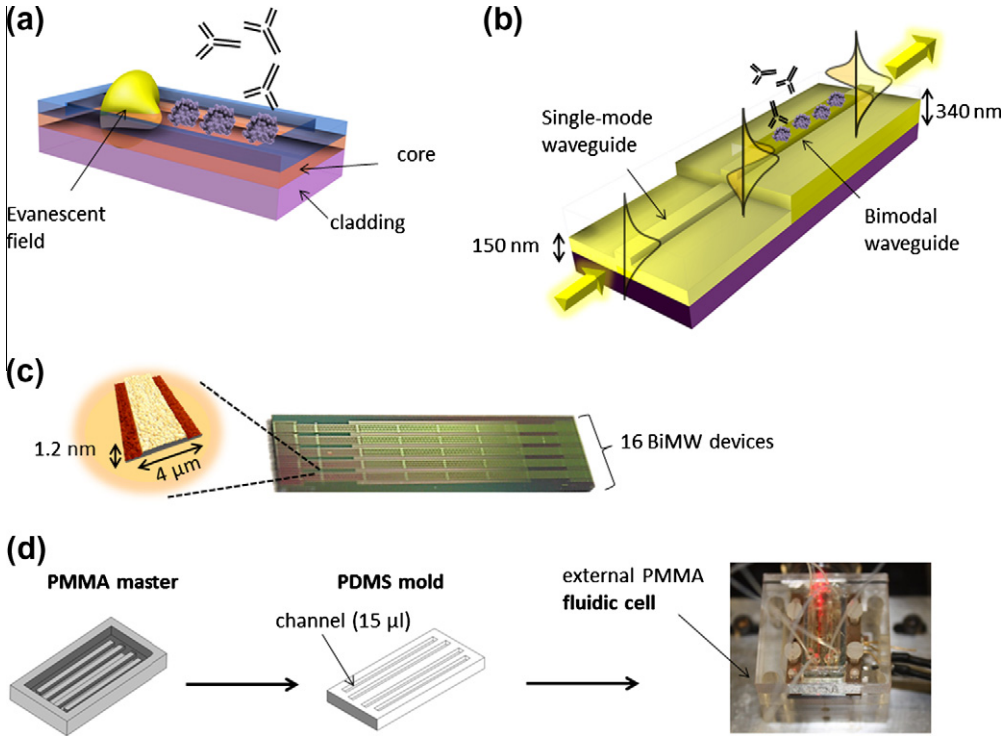

Fig. 1. (a) Scheme of the evanescent field detection principle in which the waveguide biosensors are based on, (b) interferometric operation of the BiMW device, (c) photograph of a chip consisting of 16 BiMW devices and AFM image of one rib waveguide, and (d) fabrication by soft-lithography of a PDMS mold and assembly of the fluidic cell using an external PMMA housing.

Please cite this article in press as: A.B. González-Guerrero et al., J. Colloid Interface Sci. (2012), http://dx.doi.org/10.1016/j.jcis.2012.10.040

that each one has a capacity of 15 μl and covers four BiMW sensors of the chip. The fluidic channels were fabricated in polydimethylsiloxane (PDMS) by soft lithography using a PMMA master as indicated in Fig 1d. Finally, the PDMS mold was embedded in the external PMMA fluidic cell and the tubes were bonded to the channels using PDMS as glue. Further explanations of the design, fabrication, and operation of this device can be found in [21].

To carry out the experiments, a 15 mW HeNe laser (λ = 632.8 nm) was focused at the nanometric waveguide entrance (single mode side), by using a 40× microscope objective. The fluid cell packaged chip was placed over an XYZ positioning stage, allowing the light focusing in the different BIMW sensors of the chip. The output signal (interference pattern) was collected on a two quadrant photodetector (S5870, Hamamatsu) for processing by using a digital acquisition card (National Instruments) and homemade software (Labview).

3. Results and discussion

Reaction of usual organofunctional alkoxysilanes (sketched in Fig. 2a) involves four different steps. Initially, hydrolysis of the alkoxy groups occurs. When the alkoxy groups are hydrolyzed, the condensation to oligomers takes place. After that, oligomers can form hydrogen bonding with the silanol surface that results in a covalent bond after the thermal curing [22]. After the hydrolysis, the resulting silanol groups are more electrophilic and reactive due to the electropositive structure of the silicon, which results in stronger hydrogen bonding. However, this hydrolysis turns the trialkoxyorganosilane reagent in an amphiphilic molecule that easily form vesicles, bundles, or fibers in the condensation step depending on the solvent, giving place to highly irreproducible surfaces [23]. It has been previously observed that solvents having a low dielectric constant (highly hydrophobic) can force organosilane molecules to form reversed micelles or networks or even randomly aggregated silane structures in the solution, therefore reducing the concentration of the silane head groups in the medium which prevents the self-assembled monolayer (SAM) formation [16].

Taking into account the above considerations, the silanization using an organosilane stable in water can entail several advantages if comparing with standard alkoxysilanes. The steps of hydrolysis and condensation are omitted in the silanization using CTES as it has been sketched in Fig. 2b. The clearest advantage is that the formation of a monolayer using CTES is not dependent of the changing atmospheric moisture. The alkoxy groups that protect the cross-linking of silanol groups are not required in CTES silane, due to the strong solvation of CTES molecules in water that stabilizes the solution which, in turn, prevents the polymerization of the silane molecules. Thus, after the interaction of the CTES monomers with the surface, the covalent bond including the cross-linking of silanol groups takes place after the curing process typically at 110° for 1 h [24]. In this context, using water stable silane offers several advantages such as: (i) reduction of the silane molecules polymerization, avoiding the buried of the functional groups by the carbon chains, which would make them inaccessible to the biomolecules; (ii) formation of homogeneous layers which assures a low roughness of the surface, avoiding losses of light related with the sensor surface irregularity; (iii) reduction of the distance between the transducer surface and the biomolecular event due to the formation of single layers, increasing the sensitivity of the detection, in opposition to the multilayer formation.

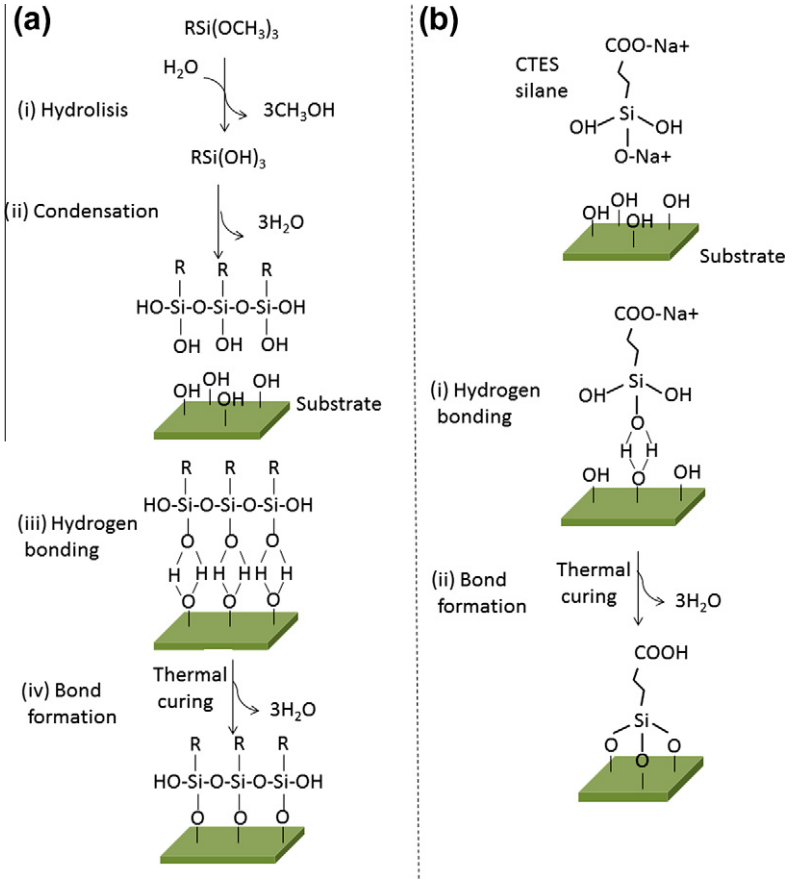

Fig. 2. Comparison between the silanization processes of surfaces using: (a) trialkoxysilane, and (b) CTES silane.

Nevertheless, there are other factors to be considered when dealing with a water stable silane. The cross-linking between silane molecules even if it is slower than in the case of trialkoxysilane is not totally avoided. We observed that for long storage period (3 months), the commercial CTES solution forms aggregates and is not useful anymore. Moreover, the thermal curing step is crucial in this silanization process to liberate water and to form the covalent bond, avoiding the hydrolysis of the siloxanes linkages. Other issues related with silanization process such as the generation of silanol groups on the Si_3N_4 surface must also be taken into account. Thus, the optimization of the sample pretreatment (cleaning and oxidizing processes) and the silanization conditions (silane concentration and immersion time) are mandatory in order to achieve the best performance of the BiMW device by using this novel silanization method. To optimize this functionalization strategy, test Si_3N_4 surfaces fabricated identically to the sensor area of our devices were employed.

3.1. Surface pretreatment

The silicon nitride surface must be accessible to oxidizing agents to create silanol groups. This aspect is critical for achieving an optimal covering with the silane molecule and, therefore, to render in highly reproducible surfaces. With this purpose, the cleaning process must ensure the total removal of contaminants with the minimal damage of the surface. Several cleaning methods are available using acid, base, organic solvents or a combination of them, as pre-treatment for the silanization [25,26]. We chose a cleaning process based on three different cleaning steps to be completely sure of the full elimination of the different types of dirtiness (dust, grease, inorganic material, etc). The first step was a standard cleaning by rinsing with acetone, ethanol, and DI water (Ac/EtOH/H_2O). In the second step, the Si_3N_4 surface was sonicated in SDS 1% and flushed with water. Finally, the sample was sonicated in HCl and MeOH 1:1 and rinsed with water. The chemical modification of the surface was checked by contact angle analysis. The values corresponding to the successive cleaning steps are shown in Table 1. Results demonstrate that the cleaning step normally employed (acetone, ethanol, and DI water) is not enough to totally remove contaminants from the surface. It can be noted a reduction in the contact angle after 5 min of sonication treatment with SDS 1% and, finally, a homogenization of the clean surface after the sonication with HCl:MeOH. These results are consistent with previous publications [25,26].

After the cleaning process, the oxidation of the Si_3N_4 surface is essential to make it reactive to the silane molecule. A layer of SiO_2 must be generated over the Si_3N_4 surface and activated to have enough silanol groups for the reaction. There is not a standard procedure for the oxidation and activation of Si_3N_4 surfaces. Several approaches have been described in the literature. For example, to directly get silanol groups several strong oxidizing cocktails have been employed such as piranha [27], a mix of ammonium chloride and HCl [28], or concentrated HNO_3 [29]. However, these aggressive solvents can damage the surface inducing an increase in the surface roughness, a drawback for waveguide devices. One alternative is using two different steps, first the incorporation of oxygen atoms to the Si_3N_4 surface using a weak oxygen plasma [30,31] or UV/ozone [32] and afterwards, the activation of this oxide by using a diluted acid solution or water [33]. This procedure will maintain the structural integrity of the optical waveguide device by minimizing the defects produced by the oxidation process on the sensor area surface. In this work, 1 h of UV/ozone was used to totally oxidize the Si_3N_4 surface, obtaining a highly hydrophilic surface with a contact angle lower than 5° which indicates the presence of ion species as O^-. After the oxidative step, a solution of 10% of diluted HNO_3 at 75 °C was employed at reflux conditions to activate the silanol groups, with a resulting contact angle of 19°.

Table 1
Contact angle measurements of Si_3N_4 surfaces after each step of the cleaning process.

Cleaning step	Contact angle (°)
N_2	45 ± 4
Ac/EtOH/H_2O	40 ± 5
SDS 1%	24 ± 6
MeOH:HCl	22 ± 1

3.2. Surface modification using a carboxyl-terminated silane (CTES)

In a wet-chemical silanization procedure, the concentration of silane and the reaction time with the surface are important parameters to obtain a stable and compact monolayer of CTES, and to avoid the formation of a multilayer structure. To study these parameters, pretreated test samples were immediately immersed in a solution of 1% of CTES silane and were allowed to react for different time periods ranging from 5 to 1200 min. Samples were then cleaned with water and placed for 1 h in an oven at 110 °C for a thermal curing step. Then, the contact angles for the different immersion times of samples in silane solution were evaluated. Values are shown in Table 2. The contact angle of silanized Si_3N_4 test surfaces reaches a maximum after 1 h of immersion in the CTES solution and decreases for longer silanization times. The pH is another important factor to control in order to avoid cross-linking; it seems that only basic pH gives packaged monolayers, probably due to the condensation of CTES silane molecules when alkoxy groups are protonated in acidic conditions.

Afterwards, we checked the applicability of this protocol for the covalent attachment of biomolecules. The covalent binding of the biomolecules over the CTES silanized surface was done through the activation of the carboxyl group by the use of EDC/NHS and the later reaction with the amino groups of the biomolecules to form a peptidic bond [34]. Thus, the previously silanized samples were activated by immersing them in an aqueous EDC/NHS solution of a molar ratio of 0.2/0.05 for 10 min. Then, the samples were rinsed with water, dried with N_2, and immersed into a solution of 50 μg/ml of BSA in PBS for 1 h. Due to the strong adsorption of BSA on the Si_3N_4 test surfaces it was necessary to clean the sample with consecutive flushing of SDS 1% and HCl 0.1 M to remove all the non-covalently attached proteins. As shown in Table 2, proteins were detached from the 20 h sample indicating that they were physically adsorbed. Thus, it can be confirmed that the total coverage of the Si_3N_4 surface was achieved with 1 h of silanization time and that longer immersion times have negative effects for the formation of the silane layer. This fact can be explained by the instability of the hydrogen bonding between the silanol groups and the CTES molecule, where silanol groups slowly come back to the silicon net and are not able to compete for a long time with the strong hydrogen bridges that form the CTES molecule with water. Thus,

Table 2
Contact angle values of silanized samples for different times using a 1% CTES solution and after immersion for 1 h in a solution of 50 μg/ml of BSA in PBS.

Time (min)	CTES (°)	BSA (°)
5	49.3 ± 3	65 ± 5
15	49.8 ± 2	–
30	55.2 ± 3	70 ± 11
60	56.6 ± 6	–
120	54 ± 5	60 ± 8
300	56.7 ± 11	70.3 ± 8
1200	43.2 ± 3	42.2 ± 8

Table 3
Contact angle values and AFM (roughness) characterization of silanized surfaces for 1 h using different silane concentrations.

CTES (%)	Contact angle (°)	Roughness (Å)
0	31 ± 1	1.5
0.2	36 ± 2	6
0.5	49 ± 1	1.2
2	47 ± 2	1

CTES molecule is detached from surface and solved again in the water for times larger than 1 h.

The concentration of CTES in the aqueous solution also plays a crucial role in the formation of a well packaged single layer of silane. Closely packed layers are effective in preventing water penetration, and have demonstrated better stability in saline environments [11]. To find the optimum silane concentration, oxidized Si_3N_4 test surfaces were placed in different concentrations of CTES solutions ranging from 0% to 2%, maintaining the silanization time fixed to 1 h. The resulting silanized surfaces were characterized by contact angle (see Table 3) and by AFM (see Fig. 3). AFM analysis reveals that a concentration of 0.2% does not totally cover the Si_3N_4 surface as it can be noted by the increase in roughness, due to the partial covering of the surface and to the length of the CTES molecule. However, the reduction of the roughness (1.2 Å) and a maximum in the contact angle (49°) indicate that a concentration of 0.5% is enough to totally cover the Si_3N_4 surface. Therefore, this contact angle value will be considered as a reference to assess the success of the silanization process when functionalizing a silicon-based device.

Once the optimal silanization conditions were found, control experiments were done to confirm the covalent binding of biomolecules over the CTES silanized surfaces, checking the surface coverage through the surface contact angle. A solution of the protein BSA was deposited onto two Si_3N_4 test surfaces, one of them was previously cleaned and silanized with CTES solution with the optimized conditions (1 h, 0.5%), while the other one was just cleaned omitting the silanization step. After, the same treatment was done on the silanized and non-silanized samples: surface activation by the use of EDC/NHS followed by immersion in a BSA protein solution, 50 μg/ml, during 1 h. After the protein incubation for both samples, silanized and bare Si_3N_4, they showed similar contact angles, 70° ± 2° and 68° ± 3°, respectively. However, after cleaning by flushing with SDS 1% followed by HCl 0.1 M, the contact angle of the non-silanized sample fell down to 40° ± 2°. On the contrary, the contact angle of the silanized surface was kept constant. These results demonstrate: (i) the detachment of non-covalently bonded protein when the sample is subjected to harsh conditions and (ii) the suitability of the silanization method for the covalent attachment of proteins.

To check the applicability of the bioconjugation protocol to the patterning of biomolecules, a biodeposition system was employed to selectively biofunctionalize the surface with FTIC-BSA. Two silanized test Si_3N_4 surfaces were employed. In one of the samples, the carboxyl groups were activated by the use of EDC/NHS, while the other one was just immersed in water after the silanization. After that, the biodeposition system was employed to pattern the samples with FTIC-BSA and allowed to react for 1 h. Then, a cleaning step was done by fluxing the sample with water. As can be seen in Fig. 4a, whereas in the carboxyl-activated sample FTIC-BSA shows a good attachment, in the non-activated sample (Fig. 4b) almost all the proteins were detached from the Si_3N_4 surface. This indicates that a covalent bonding between the carboxyl group and the FTIC-BSA has been achieved through EDC/NHS activation, whereas weak adsorption occurred on the silanized Si_3N_4 surface. The biodeposition platform was very useful in order to contrast the fluorescent spots with the surrounding surface that acts as a reference. In this experiment, we also demonstrated that the bioconjugation protocol can be combined with the selective surface patterning by using a biodeposition platform.

3.3. Application to the BiMW sensor

The final goal of this work was to apply the water–silanization protocol to attach a biological receptor layer onto the Si_3N_4 surface of a BiMW device to develop high performance biosensors. To monitor the sensor surface modification, the chip was placed in the experimental set-up after its silanization and encapsulated with the fluidic cell. After that, all the solutions needed for the activation and functionalization of the surface were flowed over the surface by injecting a constant volume of the sample into the fluid cell at a fixed flow rate. The chosen fluid channel size and flow rate ensure a laminar flow over the BiMW sensor. The progress of the biofunctionalization procedure was assessed in real-time by the analysis of the interferometric signals of the BiMW sensor. In particular, the monitoring of the bioreceptor binding to the Si_3N_4 surface provides valuable information about the efficiency of the biofunctionalization process. The interferometric signal of the covalent attachment of the BSA protein to the sensor area of the BiMW device is shown in Fig. 5a. To carry out this experiment, the BiMW chip was silanized using the CTES silane with the previously optimized protocol. Then, the carboxyl groups were activated by injecting 250 μl of EDC/NHS, immediately followed by an injection of 250 μl of BSA at a concentration of 50 μg/ml. During all the experiment a water flow was maintained at a constant rate of 20 μl/min. The interferometric signal corresponding to the binding process and/or to the change of bulk refractive index could be difficult to be interpreted by a non-experienced user. By a post-processing of this signal, it is possible to obtain an easier "common-type" graph. Values of the output signal variation (y axis) can be converted into phase signal (radians) to transform a sinusoidal signal into a linear signal (see Fig. 5b). Three different regimes can be recognized in the interferometric signal. Since the entrance of the BSA in PBS to its exit (region 1) the signal is due

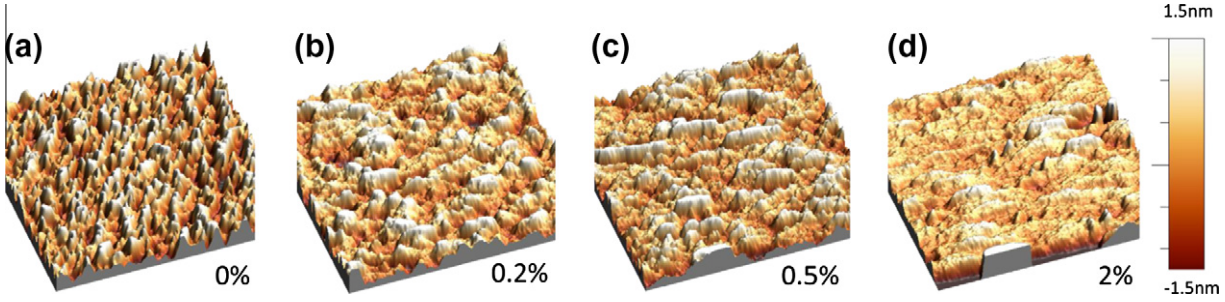

Fig. 3. AFM tapping analysis of Si_3N_4 substrates immersed for 1 h into different concentrations of CTES.

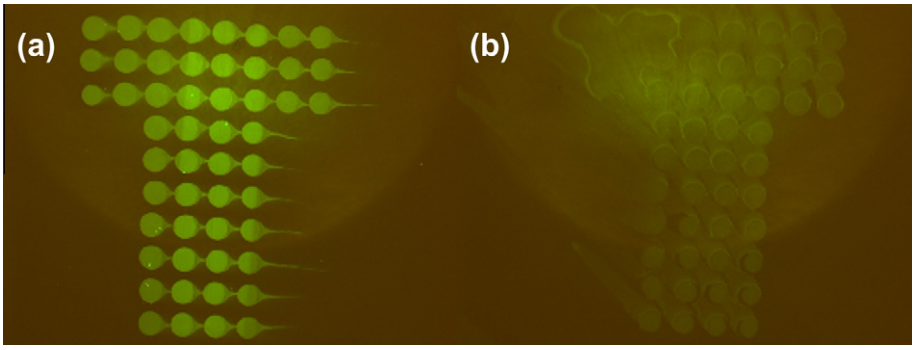

Fig. 4. Fluorescent analysis images of FTIC-BSA deposited on silanized surfaces by a commercial biodeposition system: (a) activated silanized surface and (b) non-activated silanized surface.

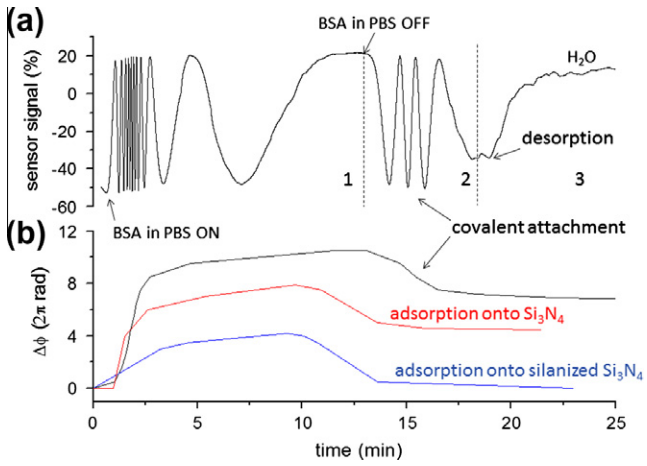

Fig. 5. (a) Real time interferometric signal of the covalent attachment of 50 μg/ml of BSA to an activated surface and, (b) signals due to the immobilization of BSA onto different surfaces (activated, silanized, and bare Si_3N_4) where interferometric graphs have been transformed into phase signals $\Delta\phi(2\pi$ rad).

to two factors: (i) the variation of bulk refractive index between the continuous water flow and the PBS containing the protein and (ii) the immobilization of the protein on the transducer surface. Afterwards, when the BSA in PBS is going out from the fluidic channel and the water is coming in, the signal is only due to the change in the bulk refractive index between PBS and water (region 2). Finally, water flow induces desorption of non-covalent attached BSA (region 3).

To investigate the non-fouling behavior of the CTES silane layer, another channel of the same silanized chip was used to evaluate the adsorption of BSA onto the silanized BiMW sensor area. In this experiment, the same conditions used for the covalent attachment were employed but the activation step was omitted. Then, 250 μl of BSA at a concentration of 50 μg/ml were flowed over the sensor area at a constant rate of 20 μl/min through the fluidic cell. The non-specific adsorption of BSA onto the silanized sensor area was negligible, as it can be seen in Fig. 5. This indicates the formation of a stable and compact silane layer and confirms that the signal obtained in the previous experiment was due to the covalent attachment. In opposition, BSA was strongly adsorbed when it was flowed over the bare sensor area of an identical BiMW device using the same experimental conditions [21]. The interferometric signal corresponding to the physical adsorption of BSA is shown in Fig. 5b for a direct comparison. The net change is larger in the case of the protein covalent attachment using the silanization procedure ($6.81 \times 2\pi$ rad) than for the direct protein adsorption over bare Si_3N_4 surface ($4.41 \times 2\pi$ rad). This indicates that the highest protein coverage is reached with the covalent strategy. The lower signal obtained for the direct adsorption of the protein can be explained by an incomplete covering of the surface, which produces a non-uniform protein layer, leaving holes that can induce the unselective adsorption of biomolecules during the biorecognition process. Moreover, strong interactions with the surface can cause conformational changes in the proteins and the consequent loose of functionality of the receptor layer, whereas weak interactions with the surface entail the possibility of desorption of the bioreceptor layer due to the liquid flow [35].

3.4. Comparison between in-flow and micro-patterning biofunctionalization strategies

For the in-flow strategy, the silanized chip was placed on the optical set-up and the solutions were flowed through the fluidic cell using the same parameters than in the previous section. On the other hand, to immobilize the biomolecules by the micropatterning strategy, the silanized chip was activated by immersion in an EDC/NHS solution for 10 min and the sensor area was filled with a mix solution of 50 μg/ml BSA and glycerol 1% by the biodeposition system and allowed to react for 1 h, at room temperature and under a 50% ambient humidity.

At this point, it is possible to evaluate the quality of the bioreceptor layers by the interferometric detection of the interaction between the specific monoclonal antibody (mAb BSA) and the immobilized BSA protein. To perform the detection, PBS was flowed at constant rate of 20 μl/min over the sensor area and a 250 μl solution of 3 nM mAb BSA was injected. After the biorecognition event, the bioreceptor surface was recovered by the use of a regeneration solution, due to the disruption of the antigen-antibody bond. A total regeneration was achieved by the injection of HCl 20 mM, allowing multiple detections using the initial state of the bioreceptor layer. The interferometric signals obtained for the biointeraction with the mAb BSA before and after the regeneration of the BSA surface, using both immobilization procedures, in-flow and patterning, are shown in Fig. 6a and b, respectively. In both cases, the response of the sensor indicates the affinity of the receptor layer for the antibody providing high selectivity to the detection. Moreover, the injection of a non-specific antibody at the same concentration (3 nM antibody against human Growth Hormone, mAb hGH) did not produce any interferometric response ($\Delta\phi 2\pi = 0$) in any of the sensor areas, in agreement with previous experiments (data not shown). The same experiment was done over the silanized sensor area where BSA was flowed, obtaining negligible signals for both specific and unspecific antibodies. These results demonstrate the specificity of the layer, the high protein receptor packaging, and the low adsorption of biomolecules over the silane layer. The regeneration of the bioreceptor layer points

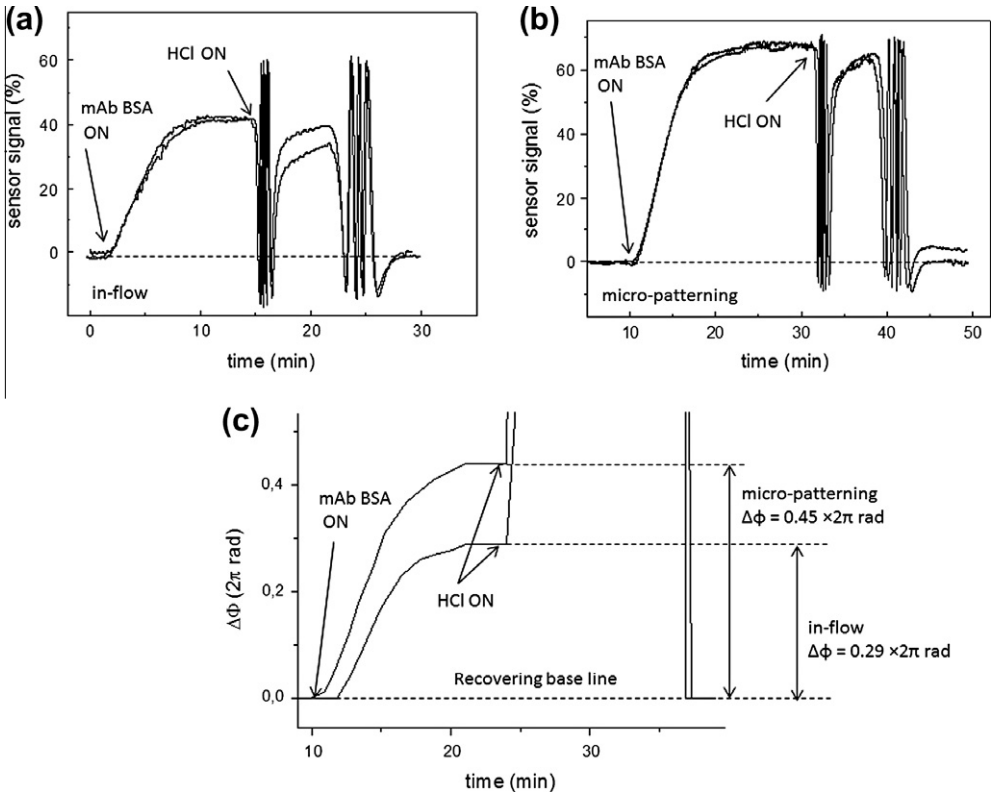

Fig. 6. Real time monitoring of the phase change due to the injection of 3 nM mAb BSA and the regeneration of the surface using both biofunctionalization strategies: (a) in-flow, (b) using the biodeposition system, and (c) comparison between both strategies (signals have been transformed into phase signals $\Delta\phi(2\pi$ rad)).

out the stability of the covalent linkage in both the silanization and the biofunctionalization procedures. However, it can be observed that the biorecognition signal when the BSA protein was immobilized using the biodeposition system ($0.45 \times 2\pi$ rad) is higher than the one obtained with the in-flow immobilization ($0.29 \times 2\pi$ rad) (see Fig. 6c). This is probably due to the reorganization capacity of the protein layer when it was allowed to react with the surface in static conditions instead of in-flow. Although selectivity and stability of the bioreceptor layer is excellent using both immobilization strategies, static conditions are preferred to enhance the signal obtained for the BiMW biosensor for a given analyte concentration due to an increase in the number of available binding sites.

4. Conclusion

The development of a functionalization strategy to covalently immobilize the bioreceptor layer in the Si_3N_4 sensor area of a novel photonic device was studied and optimized. The modification of the surface is achieved by an aqueous silanization using the CTES organosilane that provides a carboxyl group ended layer. It has been demonstrated that a complete CTES silane monolayer is assembled onto the Si_3N_4 test samples when it is used at a concentration 0.5% and for 1 h of immersion time in aqueous solution, obtaining a contact angle of 49°. The suitability of the optimized protocol for biosensing applications was checked by the real-time monitoring of the processes occurring on the sensor area of a BiMW device. Results indicate that the developed silanization protocol is highly efficient to cover the sensor area and to protect the Si_3N_4 sensor area from unspecific interactions. Two common strategies for the bioconjugation of the receptor in biosensing, the in-flow and the microdeposition patterning, were assessed for biosensing applications using the developed silanization protocol. In both cases, results indicate the high reproducibility and selectivity of the biodetection as well as the stability of the covalent attachment that allows the regeneration of the bioreceptor layer. The highest signal is obtained when the receptor layer is immobilized using the deposition system, demonstrating a better package of proteins when they are allowed to link with the silane in static conditions instead of in-flow. The results demonstrate that this water-based tethering method can be very useful to link the bioreceptor layer on different types of silicon-based devices in order to enhance its biosensing capabilities.

Acknowledgments

Authors acknowledge financial support from M. Botín foundation. The authors also would like to acknowledge Dr. Daniel Ruiz Molina and Pablo González from Nanostructured Functional Materials Group, CIN2 (Barcelona), for assistance in AFM experiments and data analysis.

References

[1] M.C. Estevez, M. Alvarez, L.M. Lechuga, Laser & Photonics Reviews 6 (2012) 463.
[2] M. Vogt, R. Hauptmann, Surface and Coatings Technology 74–75 Part 2 (1995) 676.
[3] J. Trevino, A. Calle, J.M. Rodriguez-Frade, M. Mellado, L.M. Lechuga, Talanta 78 (2009) 1011.
[4] M. Mujika, S. Arana, E. Castaño, M. Tijero, R. Vilares, J.M. Ruano-López, A. Cruz, L. Sainz, J. Berganza, Biosensors and Bioelectronics 24 (2009) 1253.
[5] A. Arafat, M. Giesbers, M. Rosso, E.J.R. Sudhölter, K. Schroën, R.G. White, L. Yang, M.R. Linford, H. Zuilhof, Langmuir 23 (2007) 6233.
[6] F. Cattaruzza, A. Cricenti, A. Flamini, M. Girasole, G. Longo, A. Mezzi, T. Prosperi, Journal of Materials Chemistry 14 (2004) 1461.
[7] A. Cricenti, G. Longo, M. Luce, R. Generosi, P. Perfetti, D. Vobornik, G. Margaritondo, P. Thielen, J.S. Sanghera, I.D. Aggarwal, J.K. Miller, N.H. Tolk, D.W. Piston, F. Cattaruzza, A. Flamini, T. Prosperi, A. Mezzi, Surface Science 544 (2003) 51.

[8] C. Haensch, S. Hoeppener, U.S. Schubert, Chemical Society Reviews 39 (2010) 2323.
[9] J. Kim, P. Seidler, L.S. Wan, C. Fill, Journal of Colloid and Interface Science 329 (2009) 114.
[10] M. Phaner-Goutorbe, V. Dugas, Y. Chevolot, E. Souteyrand, Materials Science and Engineering: C 31 (2011) 384.
[11] A. Wang, H. Tang, T. Cao, S.O. Salley, K.Y. Ng, Journal of Colloid and Interface Science 291 (2005) 438.
[12] D. Nagao, M. Yokoyama, S. Saeki, Y. Kobayashi, M. Konno, Colloid & Polymer Science 286 (2008) 959.
[13] C. Tsai, Y. Pan, C. Ting, S. Vetrivel, A.S.T. Chiang, G.T.K. Fey, H. Kao, Chemical Communications (2009) 5018.
[14] L. Han, Y. Sakamoto, O. Terasaki, Y. Li, S. Che, Journal of Materials Chemistry 17 (2007) 1216.
[15] Y. Chen, P. Xu, M. Liu, X. Li, Microelectronic Engineering 87 (2010) 2468.
[16] G. Demirel, M.O. Çağlayan, B. Garipcan, E. Pişkin, Surface Science 602 (2008) 952.
[17] S. Takayama, J.C. McDonald, E. Ostuni, M.N. Liang, P.J. Kenis, R.F. Ismagilov, G.M. Whitesides, Proceedings of the National Academy of Sciences USA 96 (1999) 5545.
[18] T.F. Didar, A.M. Foudeh, M. Tabrizian, Analytical Chemistry 84 (2011) 1012.
[19] B.H. Weigl, P. Yager, Science 283 (1999) 346.
[20] D. Samanta, A. Sarkar, Chemical Society Reviews 40 (2011) 2567.
[21] K.E. Zinoviev, A.B. González-Guerrero, C. Domínguez, L.M. Lechuga, Journal of Lightwave Technology 29 (2011) 1926.
[22] G.L. Witucki, Journal of Coatings Technology 65 (1993) 57.
[23] O.M. Martin, L. Yu, S. Mecozzi, Chemical Communications (2005) 4964.
[24] C.M. Halliwell, A.E. Cass, Analytical Chemistry 73 (2001) 2476.
[25] J.J. Cras, C.A. Rowe-Taitt, D.A. Nivens, F.S. Ligler, Biosensors and Bioelectronics 14 (1999) 683.
[26] Y. Han, D. Mayer, A. Offenhäusser, S. Ingebrandt, Thin Solid Films 510 (2006) 175.
[27] J. Diao, D. Ren, J.R. Engstrom, K.H. Lee, Analytical Biochemistry 343 (2005) 322.
[28] K.C. Popat, S. Sharma, R.W. Johnson, T.A. Desai, Surface and Interface Analysis 35 (2003) 205.
[29] R.E. Fernandez, E. Bhattacharya, A. Chadha, Applied Surface Science 254 (2008) 4512.
[30] S. Dauphas, S. Ababou-Girard, A. Girard, F. Le Bihan, T. Mohammed-Brahim, V. Vié, A. Corlu, C. Guguen-Guillouzo, O. Lavastre, F. Geneste, Thin Solid Films 517 (2009) 6016.
[31] S. Pal, M.J. Kim, J.M. Song, Lab on a Chip 8 (2008) 1332.
[32] S. Spirk, H.M. Ehmann, R. Kargl, N. Hurkes, M. Reischl, J. Novak, R. Resel, M. Wu, R. Pietschnig, V. Ribitsch, ACS Applied Materials & Interfaces 2 (2010) 2956.
[33] M. Manning, G. Redmond, Langmuir 21 (2004) 395.
[34] T.W.G. Solomons, Organic Chemistry, Wiley, New York, 1988.
[35] P. Déjardin, Proteins at Solid–Liquid Interfaces, Springer, Berlin, 2006.

Please cite this article in press as: A.B. González-Guerrero et al., J. Colloid Interface Sci. (2012), http://dx.doi.org/10.1016/j.jcis.2012.10.040